Journal of Testing and Evaluation, Vol. 41, No. 1, 2013
Available online at www.astm.org
doi:10.1520/JTE20120006

Xiaofeng Li,[1] *Zhongwei Zhang,*[2] *Lijun Qin,*[1] *Xiaoguang Yang,*[2] *Zhihai Feng,*[2] *Yang Wang,*[1] *Hong Miao,*[1] *Linghui He,*[1] *and Xinglong Gong*[1]

Measuring Mechanical Properties of the 3D Carbon/Carbon Composite Using Automated Grid Method

REFERENCE: Li, Xiaofeng, Zhang, Zhongwei, Qin, Lijun, Yang, Xiaoguang, Feng, Zhihai, Wang, Yang, Miao, Hong, He, Linghui, and Gong, Xinglong, "Measuring Mechanical Properties of the 3D Carbon/Carbon Composite Using Automated Grid Method," *Journal of Testing and Evaluation*, Vol. 41, No. 1, 2013, pp. 1–9, doi:10.1520/JTE20120006. ISSN 0090-3973.

ABSTRACT: A precise measurement, which was based on the automated grid method, was developed to analyze the mechanical properties of a three-dimensional reinforced carbon/carbon composite under tensile and shear loading conditions. Young's moduli and Poisson's ratios of the carbon/carbon composites were studied by means of unidirectional tension testing, and the shear modulus was measured using the Iosipescu shear testing technique. The contact measurement method also was applied to test the tensile strain, and a more sophisticated method based on the digital image correlation technique was applied to test the shear strain. All the testing results obtained from the different methods agree well with one another, and the analysis indicates that the automated grid method is appropriate for testing the mechanical properties of carbon/carbon composites. Based on the stress state analysis, the Young's modulus along the wrap or weft fiber orientations of the carbon/carbon composite can be obtained via the Iosipescu shear test.

KEYWORDS: carbon/carbon composites, mechanical properties, non-contact measurement method, automated grid method, Iosipescu shear test

Introduction

Three-dimensional (3D) reinforced carbon/carbon composites are one of the most promising engineering materials, and they have been widely used in the aerospace industry for, e.g., disc brakes [1–3], wing edges for space shuttles, and solid propulsion applications, as well as in many other civil industrial fields for things such as furnace tools, fasteners, nuclear reactors, biomedical implements [4], etc. This type of material displays several advantageous properties at high temperatures that lead to its outperforming many other materials; these properties include low density, low coefficient of thermal expansion, high modulus, high thermal shock resistance, high specific strength, good thermal conductivity, good toughness and friction properties, and the retention of mechanical properties at elevated temperatures. However, the application of this type of material is still restricted because knowledge about its deformation mechanism is indistinct. Considering their superior performance, more work should be done to clarify their structure dependent mechanical properties. At minimum, the precise measurement of its mechanical properties—especially the properties under tensile and shear loading—should become the first priority of studying carbon/carbon composites.

The investigation of the mechanical properties of 3D carbon/carbon composites has attracted increasing attention. In 1975, Perry and Adams did pioneering work in this area in which a conventional metal material testing method was employed to analyze the tensile properties of 3D reinforced carbon/carbon composites [5]. However, this method was limited and highly affected by the material's microstructure, heterogeneity, complex geometry, shape, size, and so on. Recently, a standard test method for measuring the mechanical properties of polymer matrix composite materials under tensile and shear loading has been defined [6,7]. However, for high modulus fiber reinforced composites, such as 3D reinforced carbon/carbon composites, this method might not be appropriate. Firstly, only a certain direction of displacement can be measured with one single strain gauge, and the full field displacement information cannot be obtained, which makes the testing of composites complicated. Secondly, the displacement measuring system will come in contact with the specimen, which leads to an effect on the measurement. Thirdly, the attachment of an extensometer or the pasting of a strain gauge will be affected by environmental and anthropic factors. Finally, the microscopic changes of the specimen cannot be observed.

Non-contact measurement methods mainly refer to all kinds of optical methods, including both interferometric techniques (such as holography interferometry, speckle interferometry, and moiré interferometry) and non-interferometric techniques (such as the automated grid method and digital image correlation). The

Manuscript received January 24, 2012; accepted for publication July 23, 2012; published online December 11, 2012.

[1]CAS Key Laboratory of Mechanical Behavior and Design of Materials, Dept. of Modern Mechanics, Univ. of Science and Technology of China, Hefei 230027, China, e-mail: gongxl@ustc.edu.cn

[2]Aerospace Research Institute of Material and Processing Technology, Beijing 100076, China.

displacements and the strains of the specimen can be determined via a numerical analysis of the digitized images of the specimen's surface with and without loading. Recently, non-contact measurement methods have been widely applied in composite materials [8,9]. Among them, the automated grid method is actively and successfully used in strain analysis for a variety of materials. In comparison with other optical methods, the advantages of the automated grid method include the less intense computational requirements for images, the feasibility of measuring large deformations, and its applicability under high temperatures. Considering the difficulty of testing 3D carbon/carbon composites, the automated grid method, which can be used as a suitable non-contact displacement measurement technique, is possibly an appropriate solution.

The grid method is one of the oldest techniques used in strain analysis [10]. For this method, a grid consisting of lines, circles, dots, or other shapes is applied on the specimen's surface before testing. The principle of the grid method is to track each spot of the undeformed and deformed images and calculate the displacements and the strains according to the differences in the spots. With the development of computer technology and solid-state video technology, the grid method became automated [11,12], increasing the testing speed and accuracy. During the past two decades, the practical application of this method has become more and more extensive. It has been successfully applied in various materials and structures, such as cracks in lamellar TiAl [13], the necking zone of a tensile specimen [14], large deformations of steel sheets [15], etc. In 2009, Lavet et al. used this method for the determination of the longitudinal Young's modulus and Poisson's coefficient of small bones. Their work pointed out a new direction for further experimental measurements of bone's mechanical properties [16]. However, the automated grid method has not been applied to analyze 3D carbon/carbon composites.

In this study, the mechanical properties of a 3D reinforced carbon/carbon composite under tensile and shear loading conditions at room temperature were measured and evaluated by means of combining the mechanical test and the automated grid method together. Six tensile specimens of carbon/carbon composites were tested using the automated grid method and the contact measurement method separately to measure the Young's moduli and Poisson's ratios of carbon/carbon composites. The two methods were compared and evaluated. Then, three types of shear specimens were tested using a combination of the Iosipescu shear test and the automated grid method, and the shear moduli were compared with results obtained using the digital image correlation (DIC) technique.

Experimental

Materials

The 3D carbon/carbon composite consisted of T-300 carbon fiber and pyrocarbon. Figure 1 schematically shows the 3D weave structure. The continuous fibers are periodically disposed along three orthogonal directions of space denoted by 1, 2, and 3, with direction 1 and direction 2 being equivalent. The material direction 1 is defined as parallel to the wrap fibers, the material direction 2 is parallel to the weft fibers, and the material direction 3 is

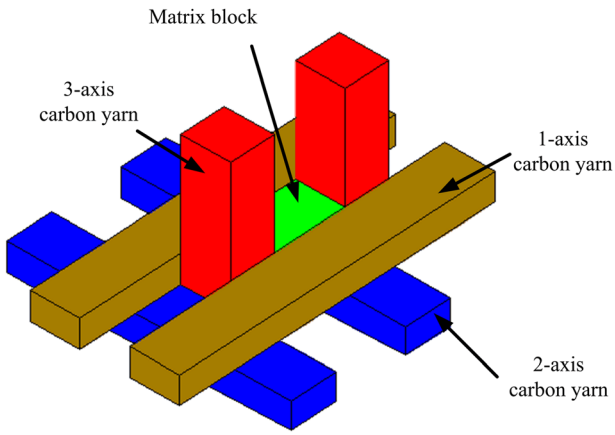

FIG. 1—*The structures of 3D carbon/carbon composites studied.*

the through-thickness direction. The nominal proportions of the fibers along directions 1, 2, and 3 are 2:2:1, respectively.

Tensile Test

The tensile testing was conducted on an MTS 809 universal testing machine (MTS Systems Corporation, Eden Prairie, MN) at a constant cross-head rate of 0.015 mm/min. For comparison, the contact measurement method was also applied to test the tensile strain. An extensometer with a measuring range of 16 % and precision of 0.5 % was attached to the back of the specimen to measure the strain response.

The specimens were machined out of consolidated plaques in accordance with GB/T 1447-2005 specimen type 1 dimensions [17]. Aluminum tabs 2 mm thick were bonded to the specimen at both ends using film adhesive. The specimen configuration is shown in Fig. 2.

Shear Test

The shearing mechanical properties were determined via the Iosipescu shear test according to ASTM D5379 [7]. For the shear testing of composites, several testing methods have been developed and studied, such as tests for the torsion of a rod with circular cut-outs, the double-notch shear test, the two-rail shear test, the shear test of rectangular prisms at 45°, torsion testing of a straight rod, torsion testing of a thin-walled tube, the square plate twist test, the Iosipescu test, etc. [18]. For composites, the Iosipescu

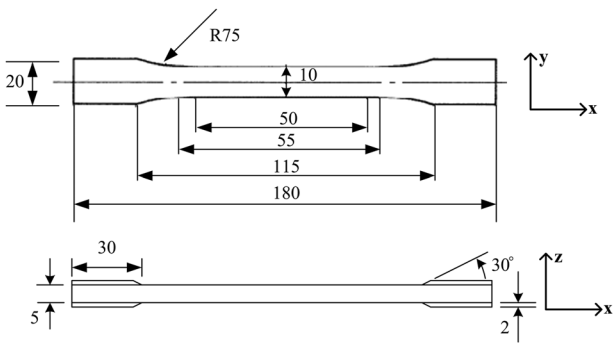

FIG. 2—*The configuration of the tensile test specimen (dimensions in millimeters).*

shear test is a better choice than other methods because of several merits. Firstly, this method can measure both the shear strength and the shear modulus of both anisotropic and isotropic materials [19]. Secondly, the shear state of the specimen is more ideal with this method. Thirdly, the specimens have a simple shape and are easy to process, which makes the experiment costless.

The loading fixture used for the Iosipescu shear test in this investigation was established by Walrath and Adams in 1977 and is known as the modified Wyoming fixture [19]. For this fixture, when two counteracting force couples are applied to the specimen, a state of pure shear stress between the notches can be produced. The specimen is symmetrical about the cross-section, and the loadings are antisymmetrical about the cross-section. According to the theory of the mechanics of materials, the specimen only sustains shear stress in the cross-section. At the same time, the bending moment is zero, which ensures a pure shear stress state.

However, a defect of this fixture is the unequal shear strain between the front and back of the specimen due to the twisting that occurs when the load is applied. Twisting occurs because of an out-of-tolerance fixture, instability of the specimens (too thin), improper installation in the fixture, out-of-tolerance conditions because of poor specimen preparation, or a material configuration with an extremely low tolerance to twist [7]. In order to eliminate this effect, the transverse is restricted by screws, and two steel blocks are introduced between the screws and the surface of the specimen to reduce the contact stress. In this case, the deformation of twist can be lessened effectively. Also, the shear strains on the front and the back of the specimen can be measured at the same time. They are averaged for the calculation of the shear modulus, which can offset the effect of twist [20].

The shear test was performed using an MTS 809 universal testing machine with a crosshead speed of 0.05 mm/min. The specimens were cut from consolidated composite plaques of the appropriate orientation in accordance with ASTM D5379 [7]. The specimen dimensions are given in Fig. 3.

Automated Grid Method

The automated grid method measurement system consists of a CCD video camera and a personal-computer-based image-processing system tracking the spot locations through automatic pattern recognition of the undeformed and deformed images. The full field displacement distribution can be calculated according to the difference in the centroid of each spot. The implementation process of the automated grid method mainly includes segmentation, calculation of the centroid coordinates, pattern recognition, and motion analysis.

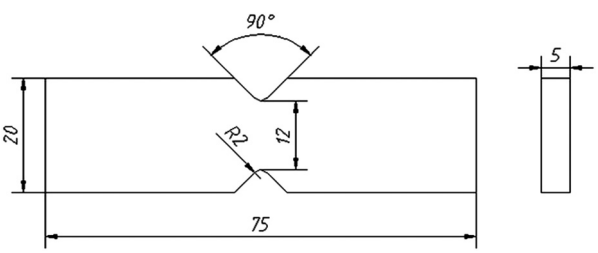

FIG. 3—*The configuration of the shear test specimen (dimensions in millimeters).*

Segmentation, consisting of identifying regions and boundaries of interest in the image, is processed by considering a threshold. The appropriate threshold is decided according to the Otsu threshold method [21]. Any level below the threshold is considered as black, so the spot size can be defined. The centroid coordinates are calculated through the image [22]. Each spot's context is uniquely determined by its position relative to its neighbors. After the context mapping, the motion analysis is continued according to the centroid coordinate of each spot.

For the tensile test, the strain was calculated through two separated spots that had an appropriate distance between them. Nevertheless, for the shear test, the strain calculation was complicated because the distribution of the shear strain was uneven. In order to solve this problem, a fitting method was adopted. First, the displacements of the test area (center area) were cubic fitted, and then the function of shear strain could be calculated by deriving the displacement function. Finally, the shear strain of the test was calculated.

A computer generated image of a 1×9 spot pattern was used for calculating the precision of the automated grid method. The picture of the spot pattern was stretched quantitatively by a computer, generating a displacement of between 0 and 1 pixels for each spot, and then the displacements were calculated by the computer program. Figure 4 schematically shows the theoretical values and the calculated values of the displacement. As shown in the figure, the precision of the automated grid method is about ± 0.02 pixels.

The conversion relation of the precision between the pixel and the displacement is as follows:

$$\Delta l = \frac{\Delta p}{p} l \tag{1}$$

where:

l = gauge length,

p = pixel of the gauge length in the picture, and

Δp = precision of the automated grid method.

In this work, the resolution of the CCD is 1280×960 pixels, and the actual length of 1 mm is equal to 40 pixels in the picture. In the experimental process, the gauge length l is taken as 20 mm;

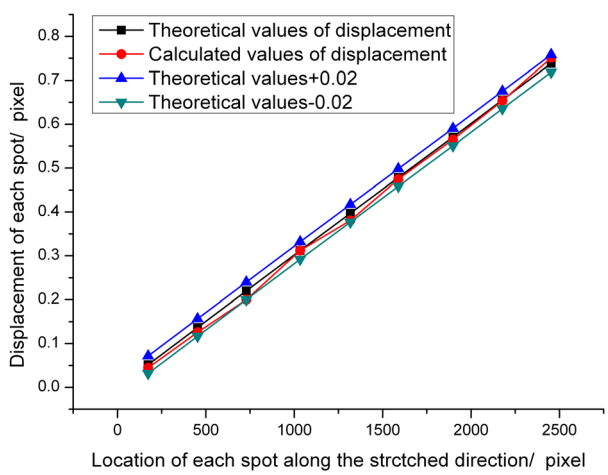

FIG. 4—*Theoretical values and calculated values of the displacement.*

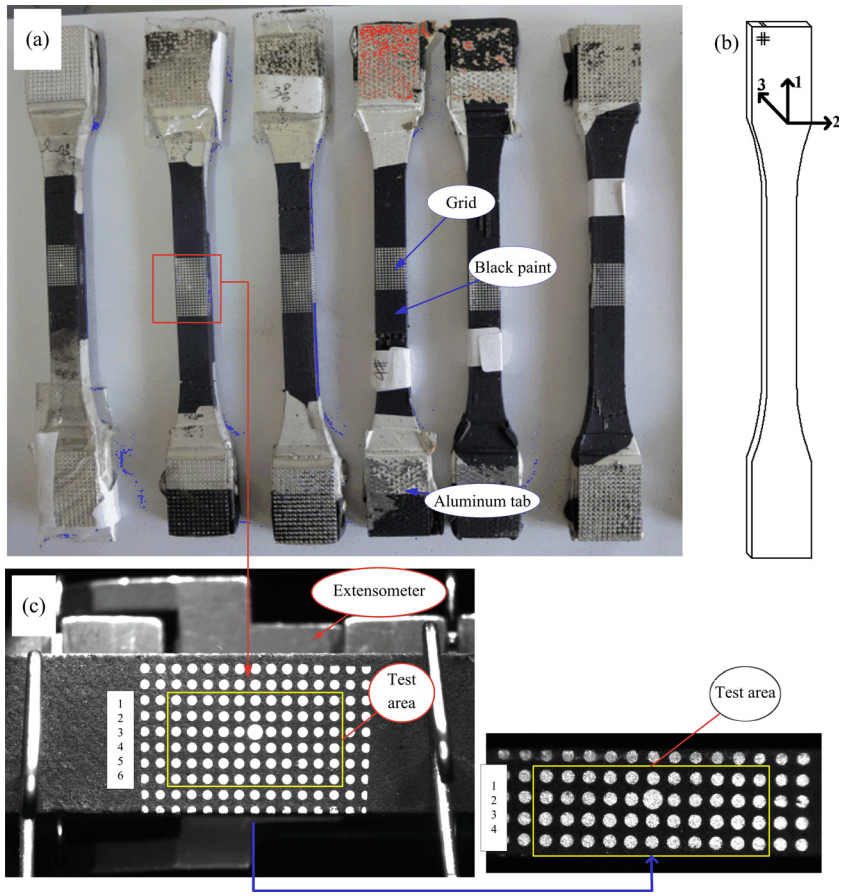

FIG. 5—*(a) Tensile specimen of carbon/carbon composite. (b) Tensile specimen orientations. (c) Spot pattern of composite tensile specimen.*

thus the pixel count of l is 800 pixels. So the precision of the displacement can be calculated as follows:

$$\Delta l = \frac{0.02}{800} \times 20\,\text{mm} = 0.5\,\mu\text{m} \tag{2}$$

which indicates that the precision of this method is superior to that of the extensometer (1 μm).

Preparation of Spot Pattern

The quality of the grid affects the precision of the automated grid method seriously. Therefore, making an appropriate grid becomes an important task. In this work, many grid-making methods were tried, and the painting-coating method was finally selected for its superiority and wide applicability. Using this method, the appropriate grids can be obtained.

The painting-coating method is divided into the following steps: first, make a piercing grid template; second, paint the specimen with black paint and put a flat base on the surface; third, align the template with the specimen closely; and finally, coat aluminum onto the surface of the specimen in an evaporation coating machine.

Procedure

For the tensile test, the grids of samples were prepared on both the front and the side in order to get the strain information in the x, y, and z directions. The x, y, and z directions correspond to the loading direction, the width direction, and the thickness direction, respectively. The sample should be fixed on the testing machine, perpendicular to the ground.

Two optical setups were established in the front and side of the texture. An optical setup included a computer, a 1 megapixel CCD, a telecentric lens, and a set of fixing devices. The deformation information of the side was measured through a 45° reflector. The lens axis was perpendicular to the sample's surface. A uniform light at each surface was ensured by lamps. When the loading was applied, pictures of the specimen from both the front and the side were recorded simultaneously.

For the shear test, the grids of the samples were prepared on both the front and the back, so as to obtain shear strains on both

TABLE 1—*Averaged Young's moduli of each surface or method.*

	Young's Modulus, GPa		
Specimen Number	Front	Side	Extensometer
1	98	111	130
2	137	115	100
3	126	119	111
4	139	125	132
5	123	122	123
6	99	107	119

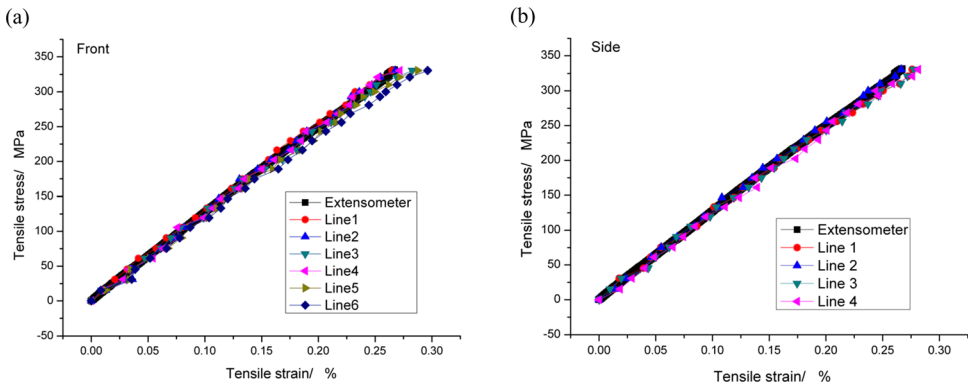

FIG. 6—*Longitudinal stress–strain relation of (a) front for specimen 5 and (b) side for specimen 5.*

surfaces of the specimen. The modified Wyoming fixture was placed on the platen of the testing machine. The same optical set-ups were used in the front and the back of the texture.

Results and Discussion

Tensile Properties

Six specimens [Fig. 5(*a*)] were tested in the tension experiment. All the specimens were cut along the 1-fiber direction [Fig. 5(*b*)], with the same geometry as given in Fig. 2. The spot pattern was put on the surface of the specimen, and the grids were prepared on both the front and side surfaces of the composite specimen so as to collect the strain information in the x, y, and z directions simultaneously [Fig. 5(*c*)]. Because the tensile stress σ_x in the x-direction is known, the Young's modulus E_x in the x direction and the Poisson's ratios μ_{xy} and μ_{xz} in the x-y and x-z planes can be obtained once the strains ε_x, ε_y, and ε_z in the x, y, and z directions are measured.

Within the testing area, a set of strain results could be calculated. There were six strain results for the front surface and four for the side surface. An extensometer was attached to the back surface of each specimen during the testing process. All the specimens were tested following the experimental conditions as mentioned before. Through an extensometer, only the global strain could be measured. In order to compare the modulus calculated by the non-contact measurement system to that obtained with the contact measurement system, the strains of each line measured by the automated grid method were averaged to get a global strain.

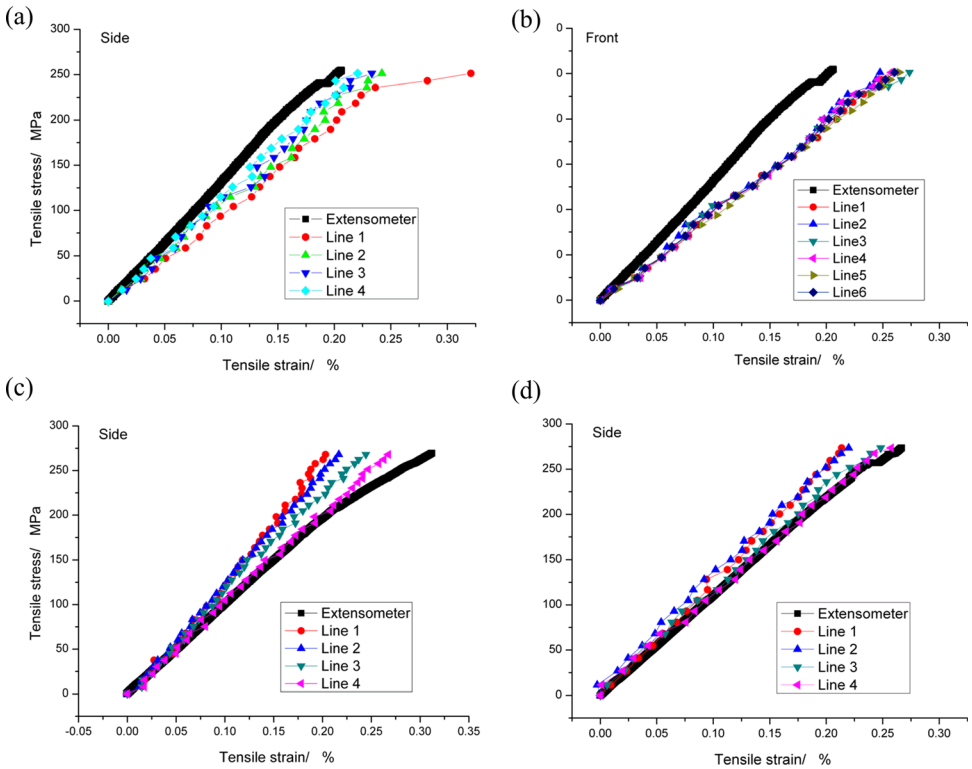

FIG. 7—*Longitudinal stress–strain relation of (a) side for specimen 1, (b) front for specimen 1, (c) side for specimen 2, and (d) side for specimen 3.*

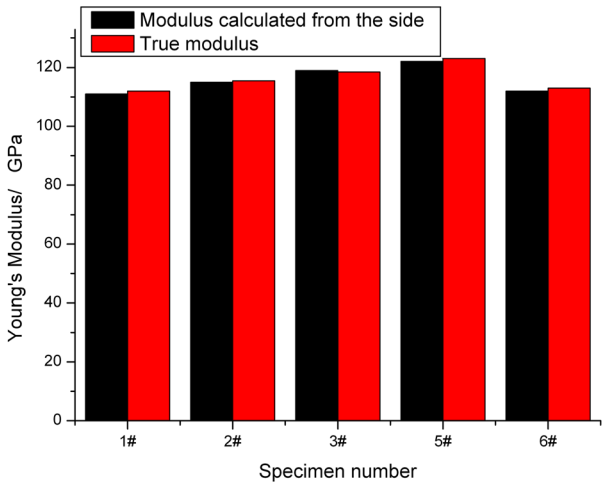

FIG. 8—*Moduli of side and true modulus for composite specimens.*

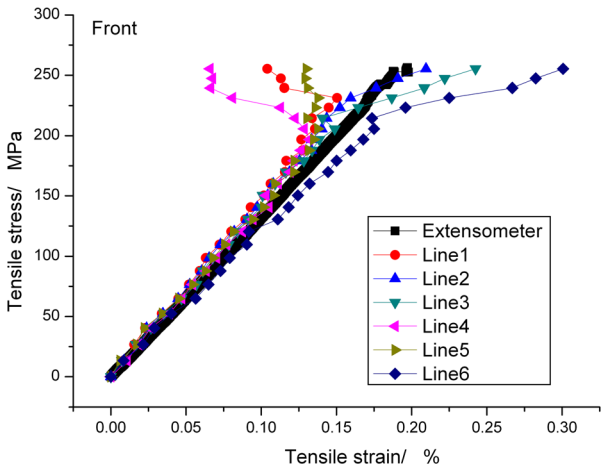

FIG. 9—*Longitudinal stress–strain relation of front for specimen 4.*

Therefore, the Young's modulus of each surface was defined as the slope of the stress–average strain curve in the initial linear region. Table 1 lists the Young's moduli of each surface or method for all the longitudinal specimens.

It can be seen that the moduli of specimen 5 calculated from the front and the side are 123 GPa and 122 GPa, respectively. These values agree well with the result calculated in the contact method (123 GPa). Also, the strains of all lines measured using the automated grid method are consistent (Fig. 6). However, for other specimens, there are some deviations in the moduli of the front and side and that measured with the extensometer. The side modulus of specimen 1 is larger than the result for the front and less than that obtained through extensometer. Specimen 6 exhibits similar behavior. In contrast, the side moduli of specimen 2 and specimen 3 are less than the results for the front and larger than those obtained through the extensometer. During the testing, the specimen not only suffered tensile loading but also suffered a bending moment that made the test specimen bend backward or forward.

When the specimen suffered a bending moment backward, the bending deformation led to increasing deformation in the front surface and decreasing deformation in the back surface, which made the modulus vary between the front and the back. From the side results of specimen 1, it can be found that the strains calculated from the line closest to the front surface decrease abruptly when the loading achieves a certain value [Fig. 7(*a*)]. This phenomenon means this area was first destroyed, leading to an expansion of the specimen. In addition, within the range of strain from 0.10 % to 0.18 %, the curves measured for the front and through the extensometer become nonlinear and symmetrically distributed with respect to the center line [Fig. 7(*b*)]. All these behaviors also indicate that the specimen had a bending deformation backward. For specimen 2 and specimen 3, the reason for the deviation was similar to the above results in that the specimen suffered a bending loading ahead. Moreover, the strain distribution of the side surface, ladder-type arranged, also supports this discussion [Figs. 7(*c*) and 7(*d*)].

From measurements of the back surface of specimen 2, it can be seen that the fracture was more serious in the back than in the front (data not shown), which means the specimen had a bending deformation ahead.

The reason for bending is mainly that the film adhesive between the aluminum tabs and the specimen cannot have a non-uniform thickness, caused by the response of the high-temperature curing treatment, which means uniaxial tensile properties cannot be achieved. This error is unavoidable during the measurement.

In consideration of the bending effect on the elastic modulus, the true value of the modulus can be calculated as follows:

$$E_{\text{true}} = \frac{\sigma_x}{(\varepsilon_{\text{front}} + \varepsilon_{\text{back}})/2} \tag{3}$$

in which $\varepsilon_{\text{front}}$ and $\varepsilon_{\text{back}}$ are the tensile strains measured from the front and the back (through the extensometer), respectively.

Therefore, if the strains of the front and the back are averaged, bending effects caused by the error can be eliminated. The true values are almost equal to the moduli taken from the side (Fig. 8). This result indicates that the moduli obtained from the deformation of the side surface are more closely related to the real value. However, the width of the specimen's side is small; thus the extensometer cannot be attached stably. In addition, the bending deformation has a bad influence on the attached extensometer.

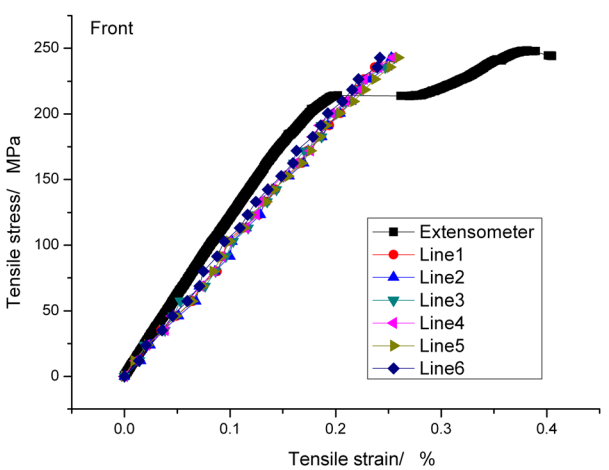

FIG. 10—*Longitudinal stress–strain relation of front for specimen 6.*

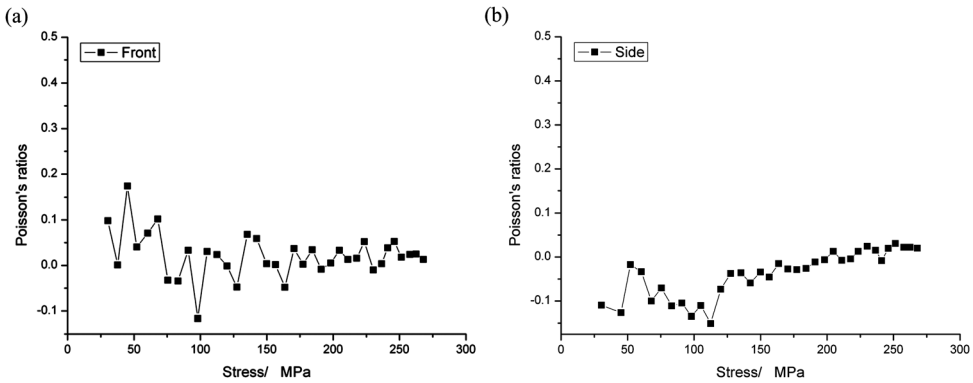

FIG. 11—*Poisson's ratios of (a) front for specimen 5 and (b) side for specimen 5.*

Therefore, the non-contact measurement method is superior to the extensometer method for tensile testing of the carbon/carbon composite.

For specimen 4, the strains of each line in the front face increased gradually from left to right (Fig. 9). When the stress achieved a critical value, the strains in each line changed sharply and suddenly. The changes in the strain from left to right appeared to have a distribution of rapid decreases to sharp increases. That behavior shows that the right side of the specimen began to fracture first because of the fault in the material. Also, the modulus calculated from the side was less than the mean of those calculated from the front and the back, because the measured strains were greater than the true strains. This phenomenon cannot be measured with the contact measurement method.

For specimen 6, when the stress achieved a certain value, the stress–strain curve measured with the contact measurement method changed to a horizontal extension (Fig. 10). A possible reason is the loose attachment of the extensometer during testing. In this case, the non-contact measurement method has superior performance.

The Poisson's ratios of the front and the side of specimen 5, μ_{xy} and μ_{xz}, were calculated using the non-contact measurement method (Fig. 11). For μ_{xy}, when the loading was relatively small, a meaningful Poisson's ratio could not be obtained, because the lateral strain was too small to be measured accurately. When the loading increased gradually, the Poisson's ratio tended to be a constant value (about 0.02) at last. According to the results, it could be calculated that the maximum lateral strains of the front surface and the side surface were less than 150 $\mu\varepsilon$. This means the maximum lateral deformation was less than 1.5 μm, so the minimum relative error was 33 % (0.5 μm/1.5 μm). Therefore, in order to obtain an accurate Poisson's ratio, the width and thickness of the specimen should be increased; this will be carried out in our future work.

As mentioned above, the Young's modulus of the carbon/carbon composite along the 1 or 2 direction is between 107 GPa and 125 GPa, and Poisson's ratio is very small (close to 0.02). Based on the above analysis, the non-contact measurement method is approved as more appropriate for tensile tests of the carbon/carbon composite.

Shear Properties

Three types of specimens, machined with different orientations, were tested [Fig. 12(*a*)]. The configuration of the specimen is given schematically in Fig. 3. The shear modulus in the 1-2 plane was obtained from specimen 1. For specimen 2, the shear modulus through the 3 direction could be calculated. Specimen 3 was used for comparisons with the tensile test.

For each specimen, grids were prepared on both the front and the back, as mentioned above [Fig. 12(*b*)]. For comparison, the DIC method was used for testing the three types of specimens. This technique requires random gray levels of the specimen's surface. This kind of distribution can be easily obtained

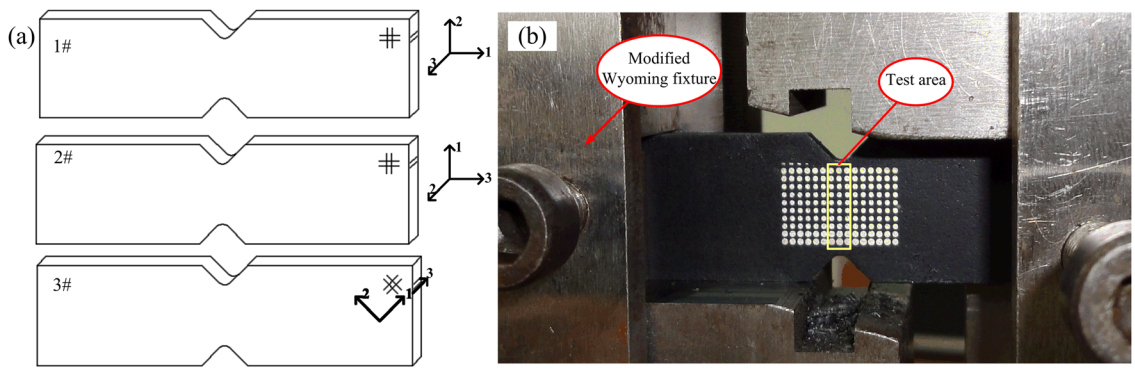

FIG. 12—*(a) Iosipescu specimen orientations. (b) Spot pattern of composite shear specimen.*

TABLE 2—*Specimen information.*

Specimen Number	Specimen Orientation	Test Method
1-1	Parallel to 1-fiber	Automated grid method
1-2	Parallel to 1-fiber	Digital image correlation method
2-1	Parallel to 3-fiber	Automated grid method
2-2	Parallel to 3-fiber	Digital image correlation method
3-1	45° to 1-fiber	Automated grid method
3-2	45° to 1-fiber	Digital image correlation method

by using black and white spray paint. The regions of interest are both the same area between the notches, as shown in Fig. 12(*b*). The complete information for the specimens is listed in Table 2.

All the specimens were tested following the experimental conditions as mentioned before. The main feature of the stress–strain curves of specimens 1 and 2 was their non-linearity, which meant a reduction of the stiffness with increasing strain. In this case, the shear moduli were calculated in the strain range of 0.02 % to 0.30 %. Moreover, the strains on the front agreed approximately with those on the back, which might be because twisting of the composite specimen was limited effectively. Here, the correct shear moduli could be calculated by averaging the strains of the front and the back.

Table 3 shows a relatively good correspondence between the results obtained using the grid technique and those obtained with the DIC one, which means these results obtained through the grid technique are credible.

Compare the results of specimen 1 to those of specimen 2; it is found that the shear modulus of specimen 2 is about 50 % or 60 % lower than that of specimen 1. The reduction might be due to the lack of fiber reinforcement in the through-thickness direction. For specimen 3, the stress–strain curves of the carbon/carbon composite showed a linear characteristic. This type of specimen gave a much higher average shear modulus than other types. This is unsurprising, because the continuous fibers at 45° can increase the in-plane shear stiffness. In addition, the Young's modulus along the 1 or 2 fiber orientation of the carbon/carbon composite can be calculated on the base of the shear modulus of specimen 3. For the tensile test, the element of the *x-y* plane is shown in Fig. 13.

Based on the stress state analysis of material mechanics, the shear stress and the shear strain on the inclined section can be calculated as follows:

TABLE 3—*Initial shear moduli of shear specimens.*

Specimen Number	Initial Shear Modulus, GPa
1-1	4.5
1-2	4.4
2-1	1.8
2-2	1.7
3-1	50.1
3-2	49.4

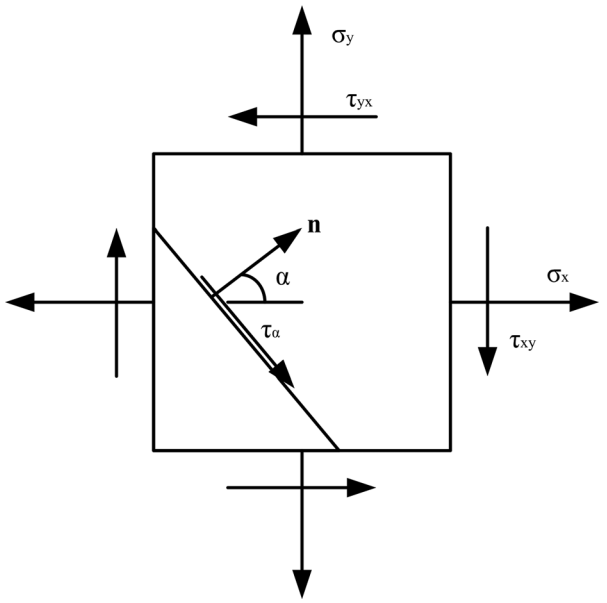

FIG. 13—*Elements of x-y plane.*

$$\tau_\alpha = \frac{\sigma_x - \sigma_y}{2}\sin 2\alpha + \tau_{xy}\cos 2\alpha$$
$$\gamma_\alpha = (\varepsilon_x - \varepsilon_y)\sin 2\alpha + \gamma_{xy}\cos 2\alpha \quad (4)$$

For the tensile test, σ_y, τ_{xy}, and γ_{xy} are equal to 0. Therefore, the shear modulus on the 45° inclined section can be calculated as

$$G = \frac{\tau_{45^\circ}}{\gamma_{45^\circ}} = \frac{\sigma_x - \sigma_y}{2(\varepsilon_x - \varepsilon_y)} \approx \frac{1}{2}E \quad (5)$$

For the above-mentioned tensile specimens, the shear modulus on the 45° inclined section has the same physical meaning as in specimen 3. Therefore, according to the shear moduli of specimen 3, the Young's modulus along the *x* direction can be calculated. It is about 100 GPa, which agrees with the results from the tensile test well (the difference between them is approximately 6.5 % to 20 %).

Conclusions

The determination of the mechanical properties of carbon/carbon composites is complex because of the material's anisotropy and heterogeneity. Current test methods for the mechanical properties might not be optimum for carbon/carbon composites, mainly because the conventional method for testing displacement, the contact measurement method, is not appropriate for this type of material. In this investigation, a precise approach for measuring the mechanical properties of carbon/carbon composites was developed on the basis of the automated grid method. Tensile and shear tests were performed using an MTS 809 material testing machine and the modified Wyoming test fixture, and the Young's modulus, Poisson's ratio, and shear modulus of carbon/carbon composites were measured. The tensile properties tested by means of the automated grid method agree well with the results measured via extensometer. The Young's modulus of carbon/carbon along the

1 or 2 direction is between 107 and 125 GPa, and Poisson's ratio is very small (close to 0.02). According to the analysis, it is found that the non-contact measurement method is more appropriate for tensile testing of carbon/carbon composites.

Three types of shear specimens, machined with different orientations, were tested. The shear moduli were compared with results obtained using a more sophisticated method based on the DIC technique, and good correspondence was obtained. The shear modulus in the 1-2 plane is about 4.5 GPa, whereas the one through the 3 direction is only 1.8 GPa. In addition, the Young's modulus along the 1 or 2 fiber orientation of carbon/carbon composites can be calculated based on a stress state analysis of material mechanics. The Young's modulus calculated through the shear test (100 GPa) matches the results from the tensile test well. Therefore, both the shear modulus and Young's modulus can be obtained through the Iosipescu shear test.

Acknowledgments

Financial support from the National Natural Science Foundation of China (Grant No. 11125210) and the National Basic Research Program of China (973 Program, Grant No. 2012CB937500) is gratefully acknowledged.

References

[1] Ruppe, J. P., "Today and the Future in Aircraft Wheel and Brake Development," *Can. Aeronautics Space J.*, Vol. 26, 1980, pp. 209–216.

[2] Hsu, S. E., Wu, H. D., Wu, T. M., Chou, S. T., Wang, K. L., and Chen, C. I., "Oxidation Protection for 3D Carbon/Carbon Composites," *Acta Astronaut.*, Vol. 35, 1995, pp. 35–41.

[3] Byrne, C., "Modern Carbon Composited Brake Materials," *J. Compos. Mater.*, Vol. 38, 2004, pp. 1837–1850.

[4] Yamamoto, O., Sasamoto, T., and Inagaki, M., "Antioxidation of Carbon-Carbon Composites by SiC Concentration Gradient and Zircon Overcoating," *Carbon*, Vol. 33, 1995, pp. 359–365.

[5] Perry, J. L. and Adams, D. F., "Mechanical Tests of a Three-dimensionally-reinforced Carbon-Carbon Composite Material," *Carbon*, Vol. 14, 1976, pp. 61–67.

[6] ASTM D3039, 2002, "Standard Test Method for Tensile Properties of Polymer Matrix Composite Materials," *Annual Book of ASTM Standards*, Vol. 15.03, ASTM International, West Conshohocken, PA.

[7] ASTM D5379, 1998, "Standard Test Method for Shear Properties of Composite Materials by the V-notched Beam Method," *Annual Book of ASTM Standards*, Vol. 15.03, ASTM International, West Conshohocken, PA.

[8] Ifju, P. G., Masters, J. E., and Jackson, W. C., "The Use of Moire Interferometry as an Aid to Standard Test-method Development for Textile Composite-materials," *Compos. Sci. Technol.*, Vol. 53, 1995, pp. 155–163.

[9] Stig, F. and Hallstrom, S., "Assessment of the Mechanical Properties of a New 3D Woven Fibre Composite Material," *Compos. Sci. Technol.*, Vol. 69, 2009, pp. 1686–1692.

[10] Parks, V. J., "The Grid Method," *Exp. Mech.*, Vol. 9, 1969, pp. 27N–33N.

[11] Sirkis, J. S. and Lim, T. J., "Displacement and Strain Measurement with Automated Grid Methods," *Exp. Mech.*, Vol. 31, 1991, pp. 382–388.

[12] Sirkis, J. S., "System Response to Automated Grid Methods," *Opt. Eng. (Bellingham)*, Vol. 29, 1990, pp. 1485–1493.

[13] Wissuchek, D. J., Mackin, T. J., DeGraef, M., Lucas, G. E., and Evans, A. G., "A Simple Method for Measuring Surface Strains around Cracks," *Exp. Mech.*, Vol. 36, 1996, pp. 173–179.

[14] Leung, Y. C., Chan, L. C., Tang, C. Y., and Lee, T. C., "An Effective Process of Strain Measurement for Severe and Localized Plastic Deformation," *Int. J. Mach. Tools Manuf.*, Vol. 44, 2004, pp. 669–676.

[15] Barone, S., Berghini, M., and Bertini, L., "Grid Pattern for In-plane Strain Measurements by Digital Image Processing," *J. Strain Anal. Eng. Des.*, Vol. 36, 2001, pp. 51–59.

[16] Lavet, C., Lapusta, Y., Toussaint, E., Labesse-Jied, F., and Poumarat, G., "On Measuring of Overall Mechanical Properties of Small Animal Bones Using Grid Method," *Int. J. Fract.*, Vol. 159, 2009, pp. 85–92.

[17] GB 1447-2005, 2005, "Fiber-reinforced Plastics Composites—Determination of Tensile Properties," Standardization Administration of China, Beijing, China.

[18] Lee, S. and Munro, M., "Evaluation of In-plane Shear Test Methods for Advanced Composite Materials by the Decision Analysis Technique," *Composites*, Vol. 17, 1986, pp. 13–22.

[19] Adams, D. F. and Walrath, D. E., "Further Development of the Iosipescu Shear Test Method," *Exp. Mech.*, Vol. 27, 1987, pp. 113–119.

[20] Morton, J., Ho, H., Tsai, M. Y., and Farley, G. L., "An Evaluation of the Iosipescu Specimen for Composite-materials Shear Property Measurement," *J. Compos. Mater.*, Vol. 26, 1992, pp. 708–750.

[21] Otsu, N., "A Threshold Selection Method from Gray Level Histograms," *IEEE Trans. Syst. Man Cybern.*, Vol. 9, 1979, pp. 62–66.

[22] Fail, R. W. and Taylor, C. E., "An Application of Pattern Mapping to Plane Motion," *Exp. Mech.*, Vol. 30, 1990, pp. 404–410.